Nonlinear Dynamical Model of Relative Motion for the Orbiting Debris Problem

Richard S. Hujsak*
Applied Technology Associates, Inc., Lionville, Pennsylvania 19341

A nonlinear dynamical model of relative motion is derived for application to the orbital breakup problem. This model is designed for analysis of debris density beginning at the time of breakup and continuing until after the cloud "rings" the Earth. A linear relative motion model is derived, which generalizes the Clohessy-Wiltshire equations to include all values of eccentricity and the secular term J_2. Then, selected higher-order terms are added, yielding generalized equations that are useful at large displacements from the reference ephemeris. A significant improvement over linear relative motion techniques is demonstrated for the expanding debris cloud. The inverse of the relative motion transformation is then shown to be an approximate solution to Lambert's problem for multiple orbits in a perturbed force field. This model enables an analysis of debris density differentially at a point in space as a function of initial breakup spread velocity statistics. Analysis is provided showing that particle density can vary by four orders of magnitude within the instantaneous cloud. Density extrema always occur at the "pinched" points of the cloud and, in a perturbed force field, also occur at discrete locations within the envelope of the expanding cloud.

Introduction

CONSIDER the problem of planning a space test where one or more vehicles will break up during collision or explosion. The test must be scheduled such that test debris does not pose a serious threat to other operational satellites. One may calculate the probability of collision between debris and each operational satellite, establish an acceptable safety threshold, and permute test conditions until all satellites are deemed safe. To compute probability of collision one needs to know the probable distribution of debris particles along the satellite's orbit path.

There have been a few attempts[1-3] to solve the near-term space safety problem. Chobotov et al.[1,2] have developed a fragmentation model that computes the spread velocity, mass, and size distribution of particles at the time of breakup as a function of the size(s) of the vehicle(s) and mass(es), while conserving momentum, mass, and energy. Fragmentation model outputs are used to find the rates of expansion of two fixed cloud shapes, one of three concentric spheres and one of concentric, pinched, truncated tori. An averaged particle density is assigned to each cloud shape, and probability of collision is measured along the path of a satellite intersecting the cloud shape.

McKnight[3] uses a fragmentation model that does not conserve momentum, mass, or energy. The fragmentation model is used to scale three fixed shapes: a hyperellipsoid, a torus, and a band about the Earth. Again, averaged particle densities (i.e., homogeneous distributions) are assigned to each shape. McKnight[3] does not actually find satellite-to-cloud intersections but computes worst case and average probabilities of collision.

These works suffer from a common problem. The authors need to predict spatial particle density from fragmentation model outputs, but fragmentation outputs are stated as probable spread velocity distributions. Techniques for rigorously predicting spatial distributions from initial spread velocity distributions do not exist. Therefore, the authors compute spatial density by computing total particles per total volume, and an empirical (geometric) shape must be assigned to determine volume.

A debris cloud is defined by the ensemble of instantaneous positions of all of the orbiting particles from a single breakup. A cloud does not conform to any specific geometric shape. Errors introduced by assuming an empirical shape lead to errors in volume and, hence, in density. Moreover, the chosen shape may not always contain the real cloud, which is unacceptable for test safety analysis. Finally, the forced assumption of average density is seriously in error. As we will show, particle density within the instantaneous cloud can vary by many orders of magnitude. Given that these problems cause errors of orders of magnitude in the probability of collision, there is a need for an improved method of calculating particle density. If the method we seek is to be verifiable, it is appropriate to seek a functional relationship between debris density and initial spread velocity that is rigorously based in dynamics.

Relative motion models have been explored[2] as a natural means of establishing the dynamical relationship we seek. Linear equations of relative motion expressed in rectangular coordinates[4] were found to be approximately correct for one quarter of an orbit following breakup, but were inadequate for the general breakup problem. Attempts to add linear perturbations have been unsuccessful in resolving the problem.

The following discussion develops a nonlinear relative motion model and evaluates the model with a simple breakup simulation. The model is shown to provide the missing dynamical relationship between spread velocity distributions and spatial density. Once that claim is established, we use the model to demonstrate that the averaged particle density can differ with the actual particle density by at least two orders of magnitude.

Linear Relative Motion Model

Model Form

A relative motion model defines motion relative to a reference ephemeris. The reference ephemeris is assumed to be generated by known analytical or numerical techniques, passing through the position of breakup at the time of breakup. The velocity of the reference ephemeris at the time of breakup can be conveniently chosen so that the reference ephemeris will always lie within the orbiting cloud. The inputs and outputs of a relative motion model normally include relative position and

Presented as Paper AAS 89-397 at the AAS/AIAA Astrodynamics Specialist Conference, Stowe, VT, Aug. 7–10, 1989; received Aug. 21, 1989; revision received Feb. 6, 1990.

*Senior Engineer, Advanced Technology Division. Member AIAA.

velocity components. Because we need a metric to define distance, and, hence, volume, we constrain inputs and outputs to rectangular Gaussian coordinates.

Linear Model Development

We seek a 6×6 transformation $\Phi^{\#1}_{t,t_0}$ that computes relative radial ΔY_1, circumferential (intrack) ΔY_2, and crosstrack ΔY_3 position and velocity components in the Gaussian frame c, defined on the reference ephemeris at time t from relative position and velocity components in the Gaussian frame b, defined on the reference ephemeris at time t_0:

$$[\Delta Y_1(t)\ \Delta Y_2(t)\ \cdots\ \Delta \dot{Y}_3(t)]_c^T = \Phi^{\#1}_{t,t_0}[\Delta Y_1(t_0)\ \Delta Y_2(t_0)\ \cdots\ \Delta\dot{Y}_3(t_0)]_b^T \tag{1}$$

Define $\Phi^{\#1}_{t,t_0}$, using the chain rule, as the product of three 6×6 transformations

$$\Phi^{\#1}_{t,t_0} = \left[\frac{\partial Y_i(t)}{\partial F_j(t)}\right]\left[\frac{\partial F_j(t)}{\partial F_k(t_0)}\right]\left[\frac{\partial F_k(t_0)}{\partial Y_m(t_0)}\right] \equiv G_1(t)\ G_2(t,t_0)\ G_3(t_0) \tag{2}$$

where F_j are orbital elements, $j=1,2,\ldots,6$. If F_j are equinoctial (a_f, a_g, n, L, χ, ψ), then $G_1(t)$ is a well-known[5] linear transformation from orbital elements to position and velocity. $G_1(t)$ is complete in eccentricity and nonsingular for all eccentricity ($0\le e<1$) and inclination ($0\le i<\pi$). $G_3(t_0)$ is simply $G_1(t_0)^{-1}$ and, likewise, nonsingular and valid for all eccentricity and inclination. $G_2(t,t_0)$ is exact for two body dynamics as

$$G_2(t,t_0) = \begin{bmatrix} 1&0&0&0&0&0\\ 0&1&0&0&0&0\\ 0&0&1&0&0&0\\ 0&0&\tau&1&0&0\\ 0&0&0&0&1&0\\ 0&0&0&0&0&1 \end{bmatrix}, \qquad \tau = t - t_0 \tag{3}$$

Formulations for $G_2(t,t_0)$ that are complete in secular J_2 already exist.[5] By adopting these existing formulations, and evaluating G_i with reference ephemeris values at times t and t_0, we claim that $\Phi^{\#1}_{t,t_0}$ is a generalization of the Clohessy-Wiltshire rendezvous equations, valid for all eccentricity and for secular J_2.

Restriction to Time of Breakup

By placing t_0 at the time of breakup, input relative positions can be set to zero. To compute debris density, the relative velocity outputs can be neglected. As a result, we are only interested in a 3×3 subset of $\Phi^{\#1}$, denoted as $\Phi^{\#2}$

$$\Phi^{\#2}_{t,t_0} = G_1'(t)G_2(t,t_0)G_3'(t_0) \tag{4}$$

where $G_1'(t)$ is a 3×6 subset of $G_1(t)$ and $G_3'(t_0)$ is a 6×3 subset of $G_3(t_0)$.

Linear Model Shortcomings

The linear transformation $G_1'(t)$ is a 3×6 matrix of dot products of the form

$$G_1'(t) = \begin{bmatrix}\hat{u}\\ \hat{v}\\ \hat{w}\end{bmatrix}\cdot\left[\frac{\partial r}{\partial a_f}\ \frac{\partial r}{\partial a_g}\ \frac{\partial r}{\partial n}\ \frac{\partial r}{\partial L}\ \frac{\partial r}{\partial \chi}\ \frac{\partial r}{\partial \psi}\right] \tag{5}$$

where r is a position vector and $\hat{u}$, $\hat{v}$, $\hat{w}$ are unit vectors in radial, intrack, and crosstrack directions, respectively. $G_1'(t)$ maps relative orbital elements into relative Cartesian position (relative to the reference ephemeris at t)

$$[\Delta Y_1(t)\ \Delta Y_2(t)\ \Delta Y_3(t)]^T = G_1'(t)[\Delta a_f(t)\ \Delta a_g(t)\ \cdots\ \Delta\psi(t)]^T \tag{6}$$

As the cloud expands, the relative orbital elements change slowly, all except relative mean longitude $\Delta L(t)$. (When the leading edge of the cloud catches the center of mass, $|\Delta L(t)|\approx 2\pi$.)

Looking ahead to the Taylor's expansion in Eq. (10), we can see that the linear transformation $G_1'(t)$ is only valid in a small neighborhood of the reference ephemeris ($|\Delta L|\ll 1$ rad). This explains why Chobotov et al.[2] report that the linear rendezvous equations are inadequate for debris cloud modeling, except for very small spread velocities or short predictions.

Nonlinear Extension

Derivation

To remove the error due to neglected higher-order partial derivatives in L, we seek a transformation Φ such that

$$\Phi_{t,t_0} = \left(G_1'(t) + G_1^*(t,\Delta L)\right)G_2(t,t_0)G_3'(t_0) \tag{7}$$

and

$$\begin{bmatrix}\Delta Y_1(t)\\ \Delta Y_2(t)\\ \Delta Y_3(t)\end{bmatrix}_c = \Phi_{t,t_0}\begin{bmatrix}\Delta\dot{Y}_1(t_0)\\ \Delta\dot{Y}_2(t_0)\\ \Delta\dot{Y}_3(t_0)\end{bmatrix}_b \tag{8}$$

where $G_1^*(t,\Delta L)$ will have the form:

$$\begin{bmatrix}\hat{u}\\ \hat{v}\\ \hat{w}\end{bmatrix}\cdot\begin{bmatrix} \displaystyle\sum_{k=2}^{\infty}\frac{\partial^k r}{\partial x L^{k-1}}\frac{1}{(k-1)!}\Delta x\,\Delta L^{k-1} & x\neq L\\ \text{or} & \\ \displaystyle\sum_{k=2}^{\infty}\frac{\partial^k r}{\partial L^k}\frac{1}{k!}\Delta L^{k-1} & x = L \end{bmatrix} \tag{9}$$

and is an explicit function of ΔL.

Omitting laborious details, each series, evaluated at $e=0$, can be determined to be an expansion of a closed-form trigonometric function of ΔL. For example,

$$\left(\sum_{k=1}^{\infty}\frac{\partial^k r}{\partial L^k}\left(\frac{1}{k!}\right)\Delta L^k\right)_{e=0} = a\hat{u}\left[-\frac{\Delta L^2}{2!}+\frac{\Delta L^4}{4!}-\frac{\Delta L^6}{6!}+\cdots\right] + a\hat{v}\left[\Delta L - \frac{\Delta L^3}{3!}+\frac{\Delta L^5}{5!}-\cdots\right] \tag{10}$$

Therefore,

$$\left(\sum_{k=2}^{\infty}\frac{\partial^k r}{\partial L^k}\left(\frac{1}{k!}\right)\Delta L^{k-1}\right)_{e=0} = \frac{a}{\Delta L}\left\{\hat{u}(-1+\cos\Delta L) + \hat{v}(-\Delta L+\sin\Delta L)\right\} \tag{11}$$

Let $G_1^*(t,\Delta L)\equiv[g_{ij}]$, $i=1,2,3$, and $j=1,\ldots,6$. Then,

$$g_{11} = -g_{22} = a(-\cos L\ \sin^2\Delta L - \sin L\ \sin\Delta L\ \cos\Delta L) \tag{12a}$$

$$g_{12} = g_{21} = a(-\sin L\ \sin^2\Delta L + \cos L\ \sin\Delta L\ \cos\Delta L) \tag{12b}$$

$$g_{13} = (-2/3)(a/n)(\cos\Delta L - 1) \tag{12c}$$

$$g_{14} = a(\cos\Delta L - 1)/\Delta L \qquad (=0 \quad \text{for} \quad \Delta L = 0) \tag{12d}$$

$$g_{15} = -aw_y \sin\Delta L \tag{12e}$$

$$g_{16} = -aw_x \sin\Delta L \tag{12f}$$

$$g_{23} = (-⅔)(a/n)\sin\Delta L \tag{12g}$$

$$g_{24} = a(\sin\Delta L - \Delta L)/\Delta L \qquad (=a \quad \text{for} \quad \Delta L = 0) \tag{12h}$$

$$g_{25} = aw_y(\cos\Delta L - 1) \tag{12i}$$

$$g_{26} = aw_x(\cos\Delta L - 1) \tag{12j}$$

$$g_{31} = g_{32} = g_{33} = g_{34} = 0 \tag{12k}$$

$$g_{35} = a(1 + w_z)[\cos L - \cos(L + \Delta L)] \tag{12l}$$

$$g_{36} = a(1 + w_z)[-\sin L + \sin(L + \Delta L)] \tag{12m}$$

where w_x, w_y, and w_z are components of $\hat{w}$ resolved on an inertial basis, and a is a semimajor axis.

Simple Test of Nonlinear Extension

Consider a 97-min period, circular orbit, and a fictitious explosion at $t = 0$, with all pieces ejected at 300 m/s, isotropically. After 97-min, the cloud extends ± 43 deg in the orbit plane from the reference point. Assume there are 18 pieces of debris, use isotropic spread velocity directions to construct 18 orbital element sets and propagate each (two body) separately. Relative positions of each are calculated and plotted as truth in the attached figures (×). Figure 1 contains three projections of the same cloud and depicts the 18 locations (o) predicted by a similar subset of the Clohessy-Wiltshire rendezvous equations.[4] (In the plot of crosstrack vs radial positions, all o are at the origin and obscured by ×.) In Fig. 2, the experiment is repeated using the nonlinear transformation Φ (with $J_2 = 0$). Observe that the nonlinear extension to the linear rendezvous equations allows relative motion techniques to be applied at very large relative displacements from the reference ephemeris.

Generalization of Lambert's Problem

For purposes of this paper, we refer to the generalized Lambert problem as Lambert's problem stated for multiple orbits in a perturbed force field, restricted to elliptic motion.

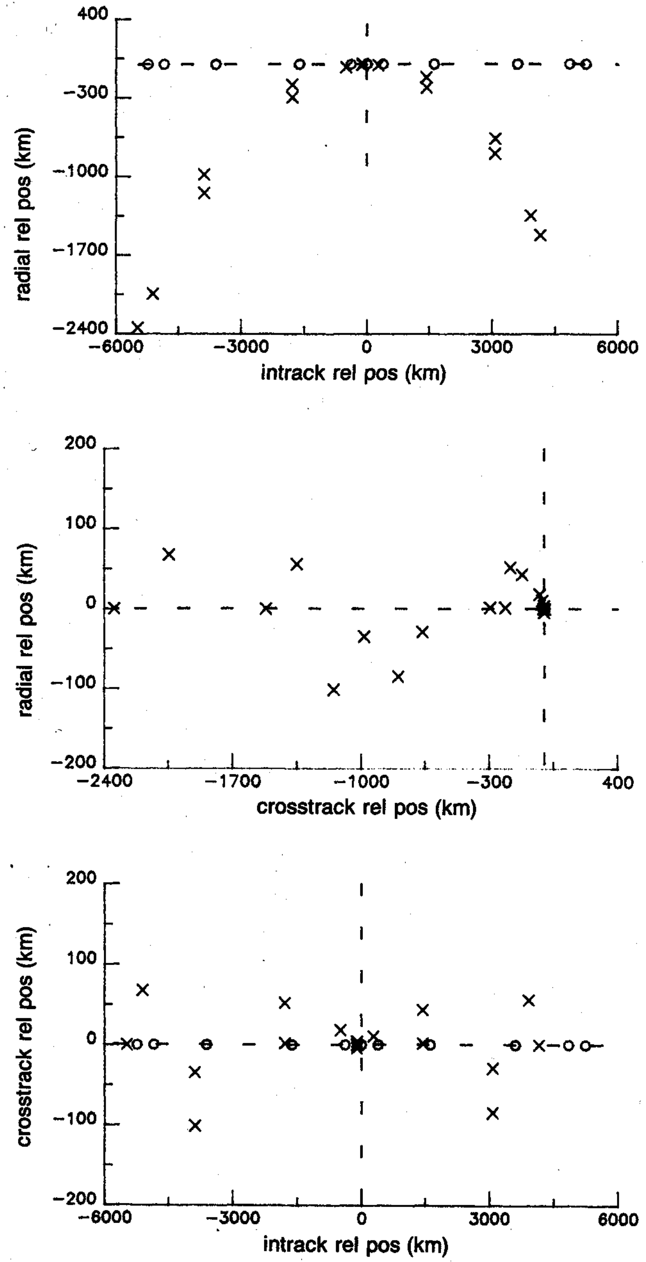

Fig. 1 Clohessy-Wiltshire predictions (o) vs actual debris locations (×).

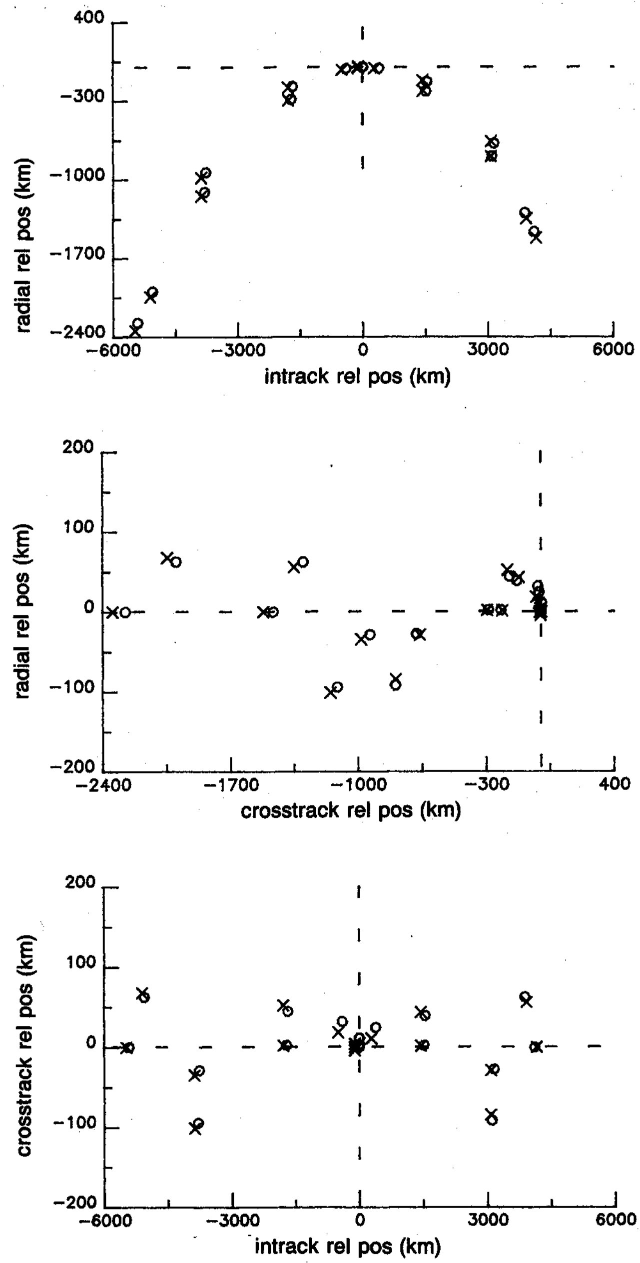

Fig. 2 Nonlinear transformation predictions (o) vs actual debris locations (×).

Accuracy of Solution to the Generalized Lambert Problem

We claim that Φ^{-1} is an approximate solution to the generalized Lambert problem. To demonstrate this claim, consider a single piece of debris, ejected from a breakup with relative velocity magnitude = 100 m/s. Compute orbital elements for this piece and generate a truth ephemeris (two body + J_2 secular). At each position in the truth ephemeris, apply Φ^{-1} to reconstruct $[\Delta \dot{Y}_i(t_0)]$. Figure 3 provides the values determined: graphed vs cloud revolutions since breakup.

Figure 3 gives evidence that Φ^{-1} is accurate to within a few percent in all three coordinates over much of space, except at multiple half-revolutions of the piece. Chobotov et al.[2] call these half-revolution and integer-revolution points pinch wedges and pinch points, places where the cloud is actually pinched through a small volume of space.

This solution to the generalized Lambert problem is singular at pinched points, just as Gauss' solution to Lambert's problem is singular at π.[6] As noted by Sun et al.,[7] the solution to Lambert's problem is not unique at each half rev. There are an infinite number of solutions to the generalized Lambert problem at the pinched points, which are not readily characterized by the transformation Φ, which is one to one. Figure 3 demonstrates that when the solution to the generalized Lambert problem is unique, Φ^{-1} provides a noniterative approximate solution that is accurate to within a few percent of the spread velocity magnitude.

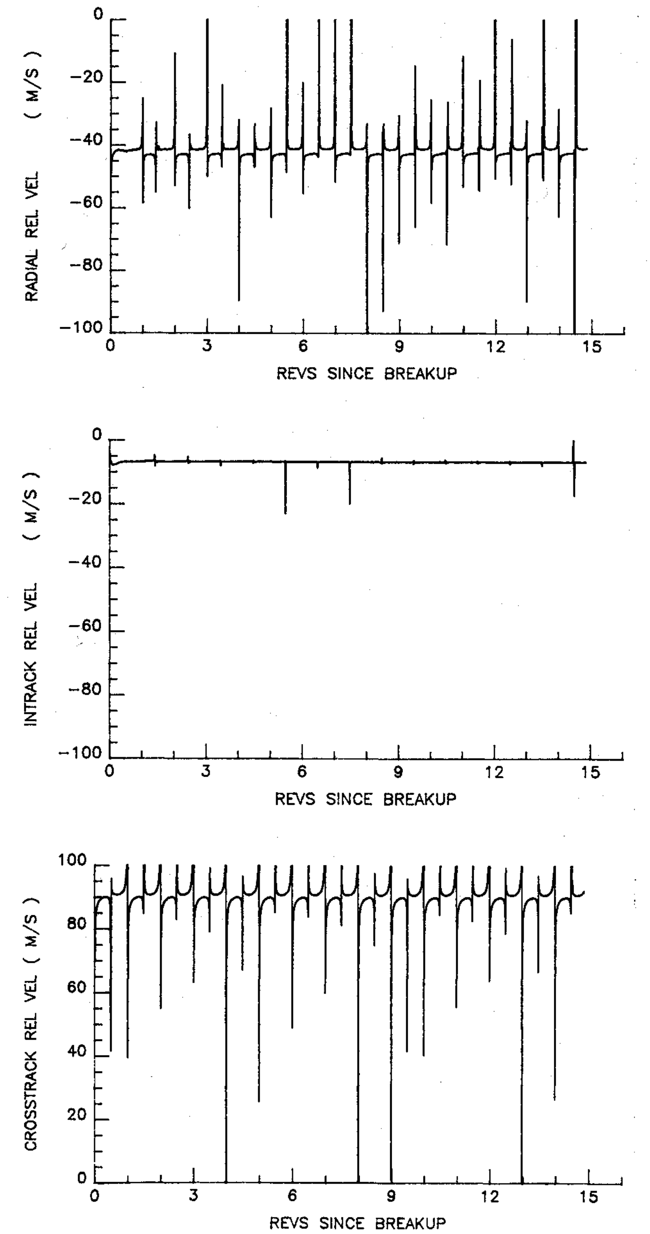

Fig. 3 Solving for breakup spread velocity using inverse nonlinear transform (case 1).

Using the Nonlinear Model to Find Debris Density

The power of the nonlinear model of relative motion is apparent when it is used to characterize debris density differentially, at some point of interest, in terms of the initial conditions of the breakup. Given the position of a satellite $r(t)$, compute $\Delta Y_i(t)$. Then apply the inverse transformation

$$\left[\Delta \dot{Y}_1(t_0)\ \Delta \dot{Y}_2(t_0)\ \Delta \dot{Y}_3(t_0)\right]^T = \Phi_{t,t_0}^{-1}\left[\Delta Y_1(t)\ \Delta Y_2(t)\ \Delta Y_3(t)\right]^T \tag{13}$$

to find an approximate solution to the generalized Lambert problem for multiple orbits in a perturbed gravity field. By adding differential increments to $\Delta Y_i(t)$ and repeating the process, we can construct a differential volume of spread velocity that maps into a differential position volume in a neighborhood of $r(t)$. If we can compute the probable number of particles in a differential velocity volume at t_0, then we know the probable number of particles in the differential position volume at t. This yields density at one point in space. Summing along the satellite path yields the probable number of particles encountered by the satellite as it passes through the cloud.

The probable number of particles in a differential velocity volume depends on the spread velocity distribution function. The trivial case is when the spread velocity distribution is homogeneous.

Example of Density Computation

For purposes of illustration, we simulate a single piece of debris ejected from a breakup with 100 m/s in the crosstrack direction. The cloud reference ephemeris is assigned a period of 97 min and assumed to be circular. The piece is found to pass through the pinch point after 97.0304 min. Φ^{-1} is repeatedly applied to find the differential volume of spread velocity that maps into a $10 \times 10 \times 10$ m^3 position volume around the piece at various times and places during the evolution of the debris cloud.

Table 1 gives the dimensions of the principal semiaxes of a quasihyperellipsoid of spread velocities at the time of breakup, which maps into a $10 \times 10 \times 10$ m^3 position volume containing the piece at the time of interest. The first column gives times since breakup, the second contains spread velocity semiaxes as determined by applying Φ^{-1}, and the third column lists the actual spread velocity semiaxes, determined by predicting an ensemble of ephemerides, each differentially deviated in initial velocity.

In Table 1, the actual spread velocity volume increases by more than four orders of magnitude near the pinched point. If the breakup spread velocity distribution is uniform in three dimensions, then the density increases by four orders of magnitude near the pinch point. For any other spread velocity distribution with the same number of particles and the same bounds, even greater density variations are possible near the pinched points.

If debris density varies by at least four orders of magnitude over a small distance within the cloud, then an averaged density hypothesis is in error by at least two orders of magnitude.

Table 1 also shows that differential velocity volumes constructed with Φ^{-1} are correct to within a few percent away from the pinch points, but degrade as one approaches the pinch point. Special case treatments are needed near the pinch points. (If we could simply constrain the intrack component of the spread velocity solution, then we would gain substantial accuracy.)

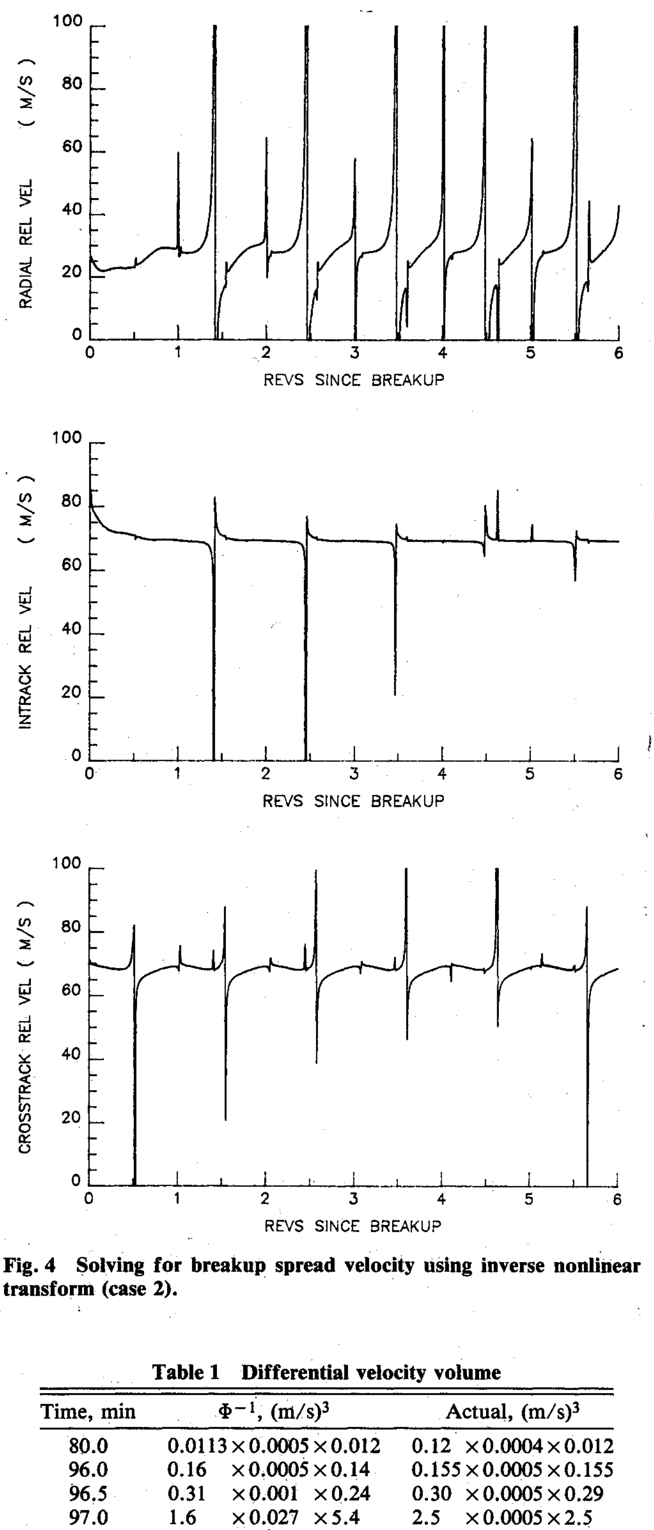

Fig. 4 Solving for breakup spread velocity using inverse nonlinear transform (case 2).

Table 1 Differential velocity volume

Time, min	Φ^{-1}, $(m/s)^3$	Actual, $(m/s)^3$
80.0	$0.0113 \times 0.0005 \times 0.012$	$0.12 \times 0.0004 \times 0.012$
96.0	$0.16 \times 0.0005 \times 0.14$	$0.155 \times 0.0005 \times 0.155$
96.5	$0.31 \times 0.001 \times 0.24$	$0.30 \times 0.0005 \times 0.29$
97.0	$1.6 \times 0.027 \times 5.4$	$2.5 \times 0.0005 \times 2.5$

Other Locations of Increased Density

The pinched locations are not the only regions of the cloud that exhibit increased particle density, although they are the most obvious. There are other locations, which occur within the envelope of the cloud, that also exhibit increased density. These are detected by repeating the experiment for Fig. 3, but assigning $\Delta\dot{Y}_1 = 26.6$ m/s, $\Delta\dot{Y}_2 = 68.8$ m/s, and $\Delta\dot{Y}_3 = 67.5$ m/s. The ability of Φ^{-1} to solve the generalized Lambert problem can be seen in Fig. 4. In addition to the singularities at the pinched locations, additional spikes occur every half revolution, well removed from the pinch point.

Φ^{-1} is nonsingular at the new spikes. Differential volume calculations performed in a neighborhood of the new spikes indicate a local increase in density by as much as four orders of magnitude.

This increased density in the debris cloud has not been detected in two-body analysis, and it is assumed that this is a manifestation of the perturbations. Apparently, perturbations yield new conditions under which the solution to the generalized Lambert problem is not unique. We can only conclude that perturbations introduce new density structures into the debris cloud, structures that are significant in terms of probability of collision analysis.

Remarks

1) The reference ephemeris can be generated with any force model appropriate to the accuracy desired, including numerical integration of a robust perturbation model.

2) $\Phi^{\#2}$ can be generated to any accuracy (e.g., by using variational equations).

3) The function $G_1^*(t,\Delta L)$ can be extended to higher-order terms in eccentricity using a Taylor series.

4) As the debris cloud rings the Earth, a single point in space $r(t)$ may be achieved by a finite number of particles, simultaneously. $G_1^*(t,\Delta L)$ is a closed-form function of sines and cosines of ΔL and can be evaluated repeatedly for $\Delta L^* = \pm n(2\pi) + \Delta L$. Particle density at $r(t)$ is the sum of differential densities obtained by repeated application of Φ for various ΔL^*. Φ effectively provides a single dynamical model of differential cloud density, valid from the time of breakup until after the cloud rings the Earth.

5) The choice of orbital elements in G_j depends on the application. Classical elements result in singularities for zero eccentricity and inclination and should be avoided. Nodal elements cannot be used for equatorial breakups, whereas equinoctial elements are nonsingular for all elliptic motion (except retrograde equatorial). Universal variables are recommended for a complete analysis of cases where elliptic and hyperbolic debris trajectories are of interest.

6) In the two-body debris problem, the pinched cloud features are fixed in inertial space at $n\pi$. For the perturbed problem, however, the pinched locations precess. The singularities in Φ^{-1} occur at the locations of the precessed pinched cloud features.

Conclusions

A nonlinear dynamical model of relative motion has been derived for application to the orbital debris problem. The model is valid for large displacements from the reference ephemeris. The linear expressions are complete in eccentricity and secular J_2, whereas the nonlinear terms are defined for zero eccentricity.

This model of relative motion can be applied successfully to compute particle density in the space safety problem. Doing so eliminates the need to assume a cloud shape, eliminates the need to use averaged particle density, and allows spatial density to be computed differentially. By treating the debris problem differentially, as a generalized Lambert problem, spatial density can be computed directly from the spread velocity distribution generated by a fragmentation model.

We have also gained considerable insight into the structure of a debris cloud. An average particle density can seriously misrepresent actual particle density. Debris density increases by at least four orders of magnitude near the pinched features of the cloud. Density also increases by four orders of magnitude, due to perturbations, at other locations internal to the cloud. Space safety analysis based on averaged particle densities may be unacceptable in light of this new result.

This model (inverse) is singular at each half rev from the breakup point and requires a complementary set of special case models to properly compute density everywhere. The required special case models do not yet exist. In the absence of these models, the relative motion model correctly identifies the locations of increased density, even though the computed densities are incorrect. Although the need for more work in this area is apparent, it is also clear that significant improvements in debris density calculations have been achieved with the chain rule, the Taylor series, and a few analytic equations from celestial mechanics. It is our fervent hope that future developments in this area attempt to improve upon this approach.

Acknowledgments

I would like to thank the U.S. Air Force for initial funding of this effort. Additionally, I wish to thank Jeannine Arsenault for observing that the nonlinear equations can be evaluated at the local value of ΔL; this proved to be the key breakthrough in this model. Jeannine Arsenault also verified all of the equations during model development. Thanks to Louis Walters, Val Chobotov, and William Sampson for review and interpretation.

References

[1]Chobotov, V. A., and Wolfe, M. G., "The Dynamics of Orbiting Debris and the Impact on Expanded Operations in Space," *Journal of Astronautical Sciences,* Vol. 38, No. 1, 1990, pp. 29–39.

[2]Chobotov, V. A., Spencer, D. B., Schmitt, D. L., Gupta, R. P., Hopkins, R. G., and Knapp, D. T., "Dynamics of Debris Motion and the Collision Hazard to Spacecraft Resulting from an Orbital Breakup," Aerospace Corporation, El Segundo, CA, SD-TR-88-96, Jan. 1988.

[3]McKnight, D., "A Phased Approach to Collision Hazard Analysis," *Advances in Space Research,* Vol. 10, No. 3/4, 1988.

[4]Clohessy, W. H., and Wiltshire, R. S., "Terminal Guidance System for Satellite Rendezvous," *Journal of Aerospace Sciences,* Vol. 27, 1960, pp. 653–658,674.

[5]Koskela, P. E., "Astrodynamic Analysis for the Advanced Orbit/Ephemeris Subsystem," Aeronutronic Ford, Newport Beach, CA, No. U4180, Sept. 1967.

[6]Battin, R. H. (ed.), *An Introduction to The Mathematics and Methods of ASTRODYNAMICS,* AIAA, New York, 1987, pp. 313–319.

[7]Sun, F., Vinh, N. X., and Chern, T., "Analytic Study of the Solution Families of the Extended Godal's Time Equation for Lambert's Problem," *Journal of the Astronautical Sciences,* Vol. 35, No. 2, 1987, pp. 213–234.